Published in final edited form as:
Curr Top Med Chem. 2013 ; 13(8): 951–962.

PET Imaging in Prostate Cancer: Focus on Prostate-Specific Membrane Antigen

Ronnie C. Mease, **Catherine A. Foss**, and **Martin G. Pomper***
Russell H. Morgan Department of Radiology and Radiological Science, Johns Hopkins Medical School, Baltimore MD, 21287, USA

Abstract

Prostate cancer (PCa) is the second leading cause of cancer-related death in American men. Positron emission tomography/computed tomography (PET/CT) with emerging radiopharmaceuticals promises accurate staging of primary disease, restaging of recurrent disease, detection of metastatic lesions and, ultimately, for predicting the aggressiveness of disease. Prostate-specific membrane antigen (PSMA) is a well-characterized imaging biomarker of PCa. Because PSMA levels are directly related to androgen independence, metastasis and progression, PSMA could prove an important target for the development of new radiopharmaceuticals for PET. Preclinical data for new PSMA-based radiotracers are discussed and include new ^{89}Zr- and ^{64}Cu-labeled anti-PSMA antibodies and antibody fragments, ^{64}Cu-labeled aptamers, and ^{11}C-, ^{18}F-, ^{68}Ga-, ^{64}Cu-, and ^{86}Y-labeled low molecular weight inhibitors of PSMA. Several of these agents, namely ^{68}Ga-HBED-CC conjugate **15**, ^{18}F-DCFBC **8**, and BAY1075553 are particularly promising, each having detected sites of PCa in initial clinical studies. These early clinical results suggest that PET/CT using PSMA-targeted agents, especially with compounds of low molecular weight, will make valuable contributions to the management of PCa.

Keywords

DCFBC; molecular imaging; positron emission tomography; PSMA; radiopharmaceutical

INTRODUCTION

Broadly defined, molecular imaging is the non-invasive detection and measurement of cellular and molecular processes in whole living beings using a variety of modalities including positron emission tomography (PET), single photon emission computed tomography (SPECT), magnetic resonance (MR), computed tomography (CT), ultrasound,

*Address correspondence to this author at the Russell H. Morgan Department of Radiology and Radiological Science, CRBII, 1550 Orleans Street, Baltimore, MD 21231, USA; Tel: 410-955-2789; Fax: 410-817-0990; mpomper@jhmi.edu.

CONFLICT OF INTEREST

The authors confirm that this article content has no conflicts of interest.

DISCLOSURE

"Part of information included in this article has been previously published in "[Current Medicinal Chemistry VOLUME: 19 ISSUE: 9 DOI: 10.2174/092986712 799462 612 <http://dx.doi.org/10.2174/092986712799462612>]" [http://www.eurekaselect.com/76655/article <http://www.eurekaselect.com/76655/article>]".

fluorescence, or bioluminescence [1–3]. Molecular imaging has become an indispensable tool in cancer research, clinical trials and medical practice. Imaging is attractive because most imaging techniques are either non- or minimally invasive, non-destructive, provide dynamic, real-time data and permit repeated measurements. Prostate cancer (PCa) is the most commonly diagnosed cancer and the second leading cause of cancer death among men in the United States [4]. Conventional imaging modalities, including bone scintigraphy (bone scan), CT, ultrasound, and MR imaging, are currently used to detect primary PCa and metastatic disease for staging and risk stratification. Current and new agents undergoing clinical study for radionuclide imaging of PCa include: 2-^{18}F-fluoro-2-deoxy-D-glucose (FDG) [5]; ^{111}In-7E11 antibody (ProstaScint™); ^{18}F-fluorodihydrotestosterone (^{18}F-FDHT) [6, 7]; radioacetate analogs [8]; radiocholine analogs [9, 10]; and *anti*-1-amino-3-^{18}F-fluorocyclobutane-1-carboxylic acid (*anti*-[^{18}F]FACBC) [11]. These agents and preclinical studies with experimental agents have been reviewed previously [12, 13], with the most clinically relevant summarized below.

FDG is an analog of glucose and is the most widely used metabolic radiotracer for PET imaging of tumors. Like glucose, FDG is transported into cells and phosphorylated but unlike glucose the phosphorylation product of FDG is trapped within the cell and accumulates. Higher glucose utilization is characteristic of most tumors, however, PCa can vary greatly in growth rate, ranging from slow-growing and less aggressive to rapidly disseminating and aggressive. As a result FDG imaging of PCa has produced mixed results. FDG was not useful in detecting primary organ-confined prostate cancer [14, 15], detecting local recurrence after radical prostatectomy, [16] or in differentiating between post-operative scar and local recurrence [16]. However, FDG is useful in detecting bone and soft-tissue PCa metastases, although it is less sensitive than bone scan [17]. It has also been shown that FDG uptake correlates with elevated prostate-specific antigen (PSA) levels and the rate of increase in PSA as a measure of metastatic disease progression [18, 19]. From these results it has been suggested that FDG is useful for imaging PCa in selected populations of patients with aggressive disease [20].

Targeted molecular imaging of PCa is best understood in the context of the first widely used, targeted agent used to image the disease, ProstaScint™. ProstaScint™, a product of EUSA Pharma, is an ^{111}In-labeled version of the monoclonal antibody 7E11 that targets the prostate-specific membrane antigen (PSMA) with the primary indication in patients with negative bone scans who are at high risk for metastatic disease, mainly within lymph nodes. ProstaScint™ has also been used to detect the site of tumor recurrence in patients with rising serum PSA. However, it is a technically demanding agent to administer [21]. Imaging generally occurs four to six days after administration of the agent, necessitating a second visit by the patient. Because it is excreted into bowel and bladder, cathartics and additional hydration are required. Blood pool imaging with ^{99m}Tc-labeled red blood cells is occasionally necessary, in order to avoid mistaking a vessel for recurrent tumor. Local extent of tumor is very difficult to interpret without concurrent SPECT/CT imaging. However, new image reconstruction algorithms provide improved image quality [22]. Because of the local inflammatory reaction in the rectum, perirectal and periprostatic regions that persist after radiation therapy, pooling of antibody can persist in these regions for years,

complicating imaging of recurrent disease. Because ProstaScint™ recognizes an internal epitope of PSMA it is believed that cells must be dead in order for them to be imaged with this agent [23]. Recently, the 7E11 antibody has been conjugated with desferrioxamine and radiolabeled with the positron emitter, ^{89}Zr ($T_{1/2}$ = 3.3 days). This agent demonstrated significantly higher uptake in PSMA-positive xenografts treated with external irradiation than in non-irradiated xenografts and suggests the use of this agent for monitoring the response to radiation therapy [24]. The J591 anti-PSMA antibody, which is directed to an external epitope on the target, has similarly been radiolabeled with ^{89}Zr, with excellent results noted in pre-clinical models and in early clinical studies [25].

^{18}F-FDHT is a radiolabeled steroid that binds to the androgen receptor (AR) utilizing a mechanism unique to PCa, i.e., expression of AR [6, 26]. It exhibits rapid and prolonged uptake in metastatic lesions [7], however, [^{18}F]FDHT is fraught with significant background within the gastrointestinal tract and liver due to enterohepatic circulation common to agents of this class.

Radioacetate analogs, as with radiocholine analogs, rely on a more general mechanism for tumor uptake, namely, fatty acid and phospholipid synthesis and metabolism. Radioacetates are therefore not cancer-specific and also accumulate in normal and hyperplastic prostate tissue [8, 20]. The relationship between the intensity of ^{11}C-acetate uptake and PSA level, a flawed but ubiquitous serum marker for PCa, remains unclear [27]. Radiocholine analogs have shown clinical promise with very early imaging, i.e, within several minutes of radiopharmaceutical administration [9, 28–31]. Rapid imaging is necessary in part due to rapid metabolism of the radiocholines, particularly ^{11}C-choline [32]. Radiocholines are not ideal imaging agents because they are flow-limited, which may present problems if used in conjunction with therapies that alter blood flow and, as noted above, they are not specific to cancer. For example, higher uptake has been demonstrated in individuals with benign prostatic hypertrophy such that in certain patients benign disease may not be differentiable from PCa [33]. Nonspecific uptake of radiocholines in granulocytes, macrophages and lymph nodes has also been described [28]. In addition radiocholines frequently display intense bowel activity.

Anti-^{18}F-FACBC is a member of a family of unnatural, alicyclic α-amino acids that exhibit anti-tumor activity [34]. The mechanism of tumor uptake is *via* amino acid transport systems including both sodium-dependent and independent transporters [35]. In humans *anti*-^{18}F-FACBC exhibited high initial uptake in liver and pancreas, which clears, and slower but prolonged uptake in skeletal muscle and bone marrow [36, 37]. Urinary excretion is low, which is advantageous for imaging primary PCa. In initial clinical studies *anti*-^{18}F-FACBC was effective in detecting both primary and metastatic PCa [11, 38].

In spite of these improvements in PCa imaging there is a need for new agents to enable accurate initial diagnosis, staging, measurement of the extent of disease upon recurrence, and therapeutic monitoring. By targeting biological mechanisms and targets unique to PCa, PET/CT may provide improvements in all four areas, especially in the latter two where disease has spread beyond the prostate gland. Because PSMA is a well characterized target for PCa and its elevated expression is associated with metastasis [39], androgen

independence [40], and progression [41], it has become a valuable focus for the development of new imaging agents, particularly for PET.

PSMA BIOLOGY

PSMA is a type II transmembrane protein that is over-expressed in PCa, including androgen-independent, advanced and metastatic disease [42–46] as well as in a few subtypes of bladder carcinoma [47], schwannoma [48], and in the tumor neovasculature of many solid tumors [49–52]. PSMA is also expressed on astrocytes where it is known as glutamate carboxypeptidase II (GCPII) and cleaves *N*-acetylaspartylglutamate (NAAG) into *N*-acetylaspartate (NAA) and glutamate [53, 54]. It is also located on the luminal side of the brush border cells in the jejunum, where it is known as folate hydrolase I, and cleaves γ-linked glutamates from folates [55, 56]. PSMA expression and localization in the normal human prostate is associated with the cytoplasm and apical side of the epithelium surrounding prostatic ducts but not basal epithelium, neuroendocrine or stromal cells [57]. Cytoplasmic PSMA is an *N*-terminally truncated form of PSMA called PSM', which has no folate hydrolase activity or capacity to hydrolyze NAAG [58–60]. It appears to be the product of post-translational modification rather than of mRNA splicing. The function of PSM' is unknown. Dysplastic and neoplastic transformation of prostate tissue results in the transfer of PSMA from the apical membrane to the luminal surface of the ducts [60, 61]. Further transformation eventually leads to expression on the plasma membrane of less differentiated epithelial cells, which is associated with the transition into and achievement of androgen growth independence [62–64]. As tumor cells advance in Gleason grade, the ratio of PSMA/PSM' reliably increases [60].

PSMA has both sequence homology and biological behavior similar to that of the transferrin receptor [65, 66]. Both receptors are membrane bound and both bind their ligands as a dimer before internalization through clathrin-coated pits [67, 68]. PSMA also exists on the membrane surface as a monomer but is enzymatically active only as a dimer [43]. Each monomer consists of a 19 amino acid cytoplasmic fragment, a 24 amino acid intra-membrane domain, and a 707 amino acid extracellular domain [68]. Following substrate binding, small-molecule antagonist or specific antibody binding, PSMA-bound ligands are internalized within the cell and are either retained in lysosomal compartments along with the degrading PSMA receptor [43], or bound ligands may be released to distribute within the cell or diffuse out of the cell as labile metabolites [69, 70]. Some internalized PSMA proteins are recycled intact back to the membrane surface through the recycling endosomal compartment (REC) [43, 71]. The cytoplasmic tail of PSMA contains consensus sequences for protein kinase C (PKC) recognition and phosphorylation. Phosphorylation of various Thr and Tyr residues by PKC may direct PSMA interaction with selected adaptor proteins, which control receptor sorting into either lysosomes or to the REC for recycling [43].

Because the expression of PSMA generally increases with increasing Gleason score [41, 62], PSMA function may be concomitant with or help facilitate malignant transformation and/or metastasis. Biological mechanisms for aiding malignant transformation or metastasis have not yet been elucidated, although PSMA-driven provision of additional folate intake as a growth advantage has been postulated [72–74].

NEW PSMA-BASED PET TMAGING AGENTS

New PSMA-based PET imaging agents fall into three categories: (1) antibodies; (2) aptamers; and, (3) PSMA inhibitors of low molecular weight. There has been a flurry of activity in each of these areas recently, particularly in the latter.

Next-Generation Antibodies

As alluded to above, J591 is a de-immunized monoclonal antibody that is specific for the extracellular domain of PSMA [75]. Unlike 7E11, which binds to an intracellular epitope, J591 binds viable cells expressing PSMA on the outer cell membrane. 1,4,7,10-Tetraazacyclododecane-N,N',N",N"'-tetraacetic acid (DOTA) conjugates of the J591 antibody have been radiolabeled with ^{111}In and ^{99m}Tc for SPECT imaging, and with ^{90}Y and ^{177}Lu for therapy [75–77]. Most recently J591 has been radiolabeled with ^{89}Zr [25 and ^{64}Cu [64] for preclinical PET imaging in mice, the former noted above.

Three murine monoclonal antibodies, 3/A12, 3/F11, and 3/E7, with specific binding to PSMA, were isolated from the spleens of mice immunized with LNCaP cell lysate [78]. DOTA conjugates of these antibodies radiolabeled with ^{64}Cu clearly delineated PSMA-positive C4-2 xenografts, [31–35% injected dose/gram (%ID/g] of tissue at 48 h post-injection], however, 3/A12 and 3/F11 conjugates also exhibited considerable uptake (11–13% of injected dose) in PSMA-negative DU145 xenografts [79]. DOTA conjugates of 3/A12 F(ab')$_2$ and Fab fragments radiolabeled with ^{64}Cu had greatly reduced tumor uptake with high kidney retention [79]. A recent abstract reports ^{89}Zr-desferrioxamine conjugates of a minibody and a cys-diabody, which demonstrate specific uptake in PSMA-positive LNCaP xenografts with a maximum uptake (6% ID/g) at 12 h, which is considerably faster than results obtained using the entire IgG [80].

Aptamers

Aptamers are either 8-15 KDa oligonucleotides or peptides isolated from combinatorial libraries, which can be selected for specific binding to target molecules through affinity maturation [81]. Their specificity and affinity for targets are similar to antibodies. They achieve their high affinity and specificity by folding into a unique three-dimensional conformation that is complementary to the surface of the target. Aptamer A10 exhibits specific binding to PSMA-positive cells *in vitro* [82]. Aptamer A10 has been used to deliver therapeutics such as doxorubicin [83] and shRNA [84–86] to PCa. The A10 aptamer has also been utilized as the PSMA targeting moiety [82, 87] for aptamernanoparticle [85, 88–92] and aptamer-quantum dot [93] conjugates. Several of these preparations, when loaded with either doxorubicin or cisplatin, demonstrated either PSMA-specific cell growth inhibition *in vitro* [85, 88, 91, 93] or tumor regression from a single intratumoral injection [89]. Recently a truncated version of aptamer A10, A10-3.2, in which the number of nucleotides has been reduced to 39 from 71, was used to prepare a polyamidoamine-polyethyleneglycol (PAMAM-PEG) conjugate for the PSMA-targeted delivery of miRNA [94]. Oligonucleotides are easily degraded and are very sensitive to changes in temperture and pH thereby complicating the preparation of radiolabeled conjugates that retain their biological activity. Recently optimized conditions for the preparation of ^{64}Cu-labeled

DOTA-, NOTA-, and 3,6,9,15-tetraazabicyclo[9.3.1]pentadeca-1(15), 11,13-triene-S-4-(4-nitrobenzyl-3,6,9-triacetic acid (PCTA)-A10 aptamer conjugates have been reported, but no *in vivo* images or biodistribution data have yet been produced using these agents [95].

Small Molecules

PSMA possesses an enzymatic site in its extracellular domain that cleaves endogenous substrates such as NAAG and poly-γ-glutamyl folic acid. The crystal structure of PSMA with and without inhibitors in the enzymatic site has been described [96–101]. The enzymatic site contains two zinc ions, and is composed of two pockets, the glutamate-sensing pocket (S1' pocket) and the non-pharmacophore pocket (S1 pocket). Most inhibitors contain a zinc binding moiety and glutamate or glutamate isostere [102] with the glutamate or glutamate isostere residing in the S1' pocket. The non-pharmacophore pocket contains an arginine rich region and can accommodate a moderately-sized lipophilic moiety. Many small molecule substrates and inhibitors for this enzyme have been prepared and tested, many prior to availability of the crystal structure of PSMA. This topic has been reviewed recently [103, 104]. A tunnel of about 20Å in length connects the binding region to the surface and acts as the front door to the active site. Another opening to the surface of the protein exists at the rear of the S1' pocket (back door). One can envision how this arrangement can facilitate the cleavage of poly-γ-glutamate substrates where the γ-glutamate enters the front door and after each individual glutamate is cleaved, exits through the back door much like spent shell casings being ejected from a firing chamber.

Small molecule PSMA inhibitors are generally zinc binding compounds attached to a glutamate or glutamate isostere and fall into three families: (1) phosphonate-, phosphate-, and phosphoramidates; (2) thiols; and, (3) ureas. Initial work on phosphonate and phosphate inhibitors, which included the potent GCPII inhibitor 2-(phosphonomethyl)pentanedioic acid, 2-PMPA [105] (Fig. 1), as well as the thiol-based GCPII inhibitors, came from research conducted at ZENECA and then Guilford Pharmaceuticals [106, 107]. Later, extensive studies with the phosphoramidate inhibitors were produced by the Berkman group [108–110]. The initial preparation and testing of urea-based inhibitors was reported by Kozikowski [111, 112]. Work with 2-PMPA and the ureas was originally geared toward inhibition of GCPII for treating neuropsychiatric disease.

Research on new imaging agents for PCa based on small molecule PSMA inhibition has concentrated on the use of either phosphoramidate or urea scaffolds. Several phosphoramidate inhibitors for optical [109, 113] and SPECT [114, 115] imaging have been reported. ^{18}F-Fluorobenzoyl phosphoramidate **1** (Fig. 1), has been prepared using the ^{18}F-labeled prosthetic group, *N*-succinimidyl 4-[^{18}F]fluoroben zoate (^{18}F-SFB) and demonstrated specific uptake in PSMA-positive LNCaP xenografts with a tumor uptake of 1.2% ID/g at 2 h post-injection. A recent abstract describes monovalent and bivalent ^{64}Cu conjugates prepared from 2-(((3-amino-3-carboxypropyl)(hydroxy)phosphoryl) methyl)pen tanedioic acid (GPI) and **2** and **3**, respectively [116] (Fig. 1). Unfortunately, the structures of the final compounds were not disclosed. The bivalent compound had 1-1.4 percentage injected dose per gram of tissue (%ID/g) tumor uptake out to 24 h, which was higher than that of the monovalent compound. In another recent abstract, Bayer Healthcare reported the

preparation of 2-PMPA analogs (2*S*, 4*S*)-2-^{18}F-fluoro-4-(phosphonomethyl) pentanedioid acid (BAY1075553) and (*2R*, 4*S*)-2-^{18}F-fluoro-4-(phosphonomethyl) pentanedioid acid **4** (Fig. 1) in a 9/1 ratio from an isomerically pure (*2R*, 4*S*)-2-tosyl precursor **5** [117]. BAY1075553 demonstated high uptake in PSMA-expressing LNCaP tumor xenografts with rapid renal clearance. Normal organ uptake was only observed in the kidneys and bladder [117].

The first radiolabeled, low molecular weight imaging agent targeting PSMA was *N*-[*N*-[(*S*)-1,3-dicarboxypropyl]carbamoyl]-*S*-[^{11}C]methyl-L-cysteine (^{11}C-DCMC) **6** (Fig. 2) [118, 119]. This was prepared by methylation of the cysteine-glutamate urea precursor **7** with ^{11}C-methyl iodide in dimethylformamide previously saturated with anhydrous ammonia. This radiotracer demonstrated site-selective uptake within PSMA-positive LNCaP tumors, showing less uptake in PSMA-negative PC-3 (prostate) and MCF-7 (breast) tumor xenografts. The 30 min LNCaP tumor uptake was 8.7% ID/g with tumor/muscle and tumor/blood ratios of 11 and 8, respectively. Although this work demonstrated the proof-of-principle for radiolabeled ureas to be used as PSMA-targeted agents for PET, an ^{18}F-labeled radiotracer, with its more tractable 110 min physical half-life was desired. To that end *N*-[*N*-[(*S*)-1,3-dicarboxypropyl] carbamoyl]-4-[^{18}F]fluorobenzyl-L-cysteine (^{18}F-DCFBC) **8** (Fig. 2), was prepared by alkylation of **7** with 4-[^{18}F]fluorobenzyl bromide [120] in methanol previously saturated with anhydrous ammonia. Using ^{18}F-DCFBC, PSMA-positive PC-3 PIP xenografts were visualized as early as 20–30 min post-injection with little radioactivity in the PSMA-negative, isogenic PC-3 flu xenografts. By 2 h the PC-3 PIP xenografts remained clearly visible with significant clearance of background radioactivity from the blood, liver and kidneys. The PSMA-positive PC-3 PIP xenograft uptake was 6.2, 8.2 and 4.7% ID/g at 30 min, 1 h, and 2 h post-injection, respectively with 2 h tumor/muscle and tumor/blood ratios of 20 and 13, respectively [121]. The radio-synthesis of ^{18}F-DCFBC has been automated and utilizes a radiochemistry microwave reactor for the preparation of 4-[^{18}F]fluorobenzyl bromide [122], followed by the room temperature reaction with **7** in tetrabutylammonium hydroxide/acetonitrile [123].

Lysine-glutamate urea **9** and its tri-ester **10** (Fig. 2) are useful scaffolds for the addition of radiofluorinated, amine-reactive prosthetic groups or linking groups to span the 20Å void to the surface of the protein. For example, compound **10** was reacted with the well known prosthetic group, ^{18}F-SFB, followed by ester hydrolysis to give **11** [124]. Compound **11** demonstrated specific uptake in PSMA-positive PC-3 PIP xenografts with 6.4 and 3.7% ID/g uptake at 1 and 2 h post-injection, respectively. The 2 h tumor/muscle and tumor/blood ratios were 18 and 9, respectively. Compound **10** has also been reacted with the recently reported prosthetic group 6-^{18}F-fluoro-nicotinic acid tetrafluorophenyl ester (^{18}F-Py-TFP) [125], followed by hydrolysis to give 2-(3-{1-carboxy-5-[(6-[^{18}F]fluoro-pyridine-3-carbonyl)-amino]-pentyl}-ureido)-pentanedioic acid, (^{18}F-DCFPyL) **12** [126]. Specific uptake in PSMA-positive PC-3 PIP xenografts was seen as early as 30 min post-injection, and by 3.5 h radioactivity cleared from all normal tissues. The 2 h uptake in PSMA-positive PC-3 PIP xenografts was 39.4% ID/g with tumor/muscle and tumor/blood ratios of 985 and 92, respectively. A recent abstract describes the preparation of MIP-1500, compound 13 [127], but no biological data are available as of this writing.

Banerjee [128] reported the preparation and testing of the first ^{68}Ga-labeled PSMA-targeted imaging agents. Compound **14** (Fig. 3) utilizes a linker that combines the suberate-lysine linker and the diphenylalanine linker previously used separately to prepare ^{99m}Tc-tricarbonyl [129] and ^{99m}Tc-oxo SPECT agents [130]. Attachment of a DOTA-3A chelator completed the structure of **14**. PSMA-positive PC-3 PIP tumors were clearly visible as early as 45 min post-injection with little visible uptake in the PSMA-negative PC-3 flu xenografts. The 2 h uptake in PSMA-positive PC-3 PIP xenografts was 3.3%o ID/g with tumor/muscle and tumor/blood ratios of 110 and 22, respectively. Eder *et al.* has prepared **15** (Fig. 4) which uses the chelator N,N'-bis[2–hydroxy-5-(carboxyethyl)-benzyl]ethylenediamine-N,N'-diacetic acid (HBED-CC), which is an analog of HBED. HBED is a potentially more attractive chelator for ^{68}Ga than DOTA because it forms a more thermodynamically stable complex than does DOTA ($\log K_{ML}$s 35.6 vs. 21.3) [131]. This study compared the biodistribution of **15** with **14** [132]. PSMA-positive LNCaP tumor xenografts were visible at 1 h post-injection using **15**. In addition, compound **15** exhibited higher uptake in LNCaP tumor xenografts, (7.5% ID/g) at 1 h post-injection than did compound **14** (4%ID/g), however, the spleen and kidney uptake values for **15** were significantly higher than for **14**. A dimer of **15**, compound **16**, where each propanoic acid moiety of HBED-CC is conjugated to a linker-lysine-glutamate urea has been reported [133]. Dimer **16** was a more potent inhibitor than monomer **15** (IC_{50} dimer = 2.1 nM; IC_{50} monomer = 9.0 nM) and demonstrated greater LNCaP tumor uptake at 1 h postinjection (4.9% ID/g for monomer **15** and 8.2%ID/g for dimer **16**). The 1 h tumor/muscle and tumor/blood ratios were 10 and 4.9 for monomer **15**, and 9 and 27 for dimer **16**, respectively.

Copper-64-labeled conjugates have also been investigated as PSMA-targeting imaging agents. The same linker-urea used in **14** was conjugated with 4,11-bis(carboxy methyl)-1,4,8,11-tetraazabicyclo[6.6.2]hexadecane (CB-TE2A), 1-oxa-4,7,10-triazacyclododecane-5-**S**-(4-isothio cyanatobenzyl)-4,7,10-triacetic acid (oxo-DO3A), PCTA, and 1,4,7-triazacyclononane-1,4,7-triacetic acid (NOTA) followed by radiolabeling with ^{64}Cu to give compounds **17**-**20**, respectively (Fig. 3) [134]. All of the ^{64}Cu-labeled conjugates demonstrated high uptake in PSMA-positive PC-3 PIP tumor xenografts, with **18** (the oxo-DO3A conjugate) having the highest tumor uptake (38.5% ID/g) at 2 h post-injection. The CB-TE2A conjugate **17** had the fastest background clearance, which provided the best tumor-to-background ratios.

Yttrium-86 ($T_{1/2}$ = 14.7 h) is a positron emitter that can be used as an imaging-based stand-in for the pure beta emitter ^{90}Y in preclinical studies. Yttrium-86 DOTA-3A and SCN-Bn-DOTA conjugates **21** and **22** (Fig. 3) have been prepared [135]. Both agents displayed high specific uptake in PSMA-positive PC-3 PIP tumor xenografts, where DOTA-3A conjugate **21** exhibited faster normal organ clearance. Based on the promising results with compounds **14**-**22** and the corresponding fluorescent agents synthesized using the lysine-glutamate scaffold **9** [136], it appears that species of substantial size can be conjugated to **9** with retention of PSMA targeting, if a sufficiently long linker is used. In fact, long chained polyethylene glycol (PEG) units have been conjugated to **9** to provide PSMA targeting for nanoparticles [137, 138].

2-[3–1,3-dicarboxypropyl)ureido]pentanedioic acid (DUPA) (Fig. 5), and its tri-ester derivative, are also useful scaffolds for the preparation of PSMA-targeted imaging agents including those for SPECT and potentially for optical imaging [130, 139]. An optimized radiosynthesis of DUPA analog **23**, using (^{18}F-Py-TFP) [125], has been reported but *in vivo* data are not available [136]. The same group has also described the high-yield radiosynthesis of [Al^{18}F]NOTA-linker-DUPA, but *in vivo* data are currently unavailable [140].

^{18}F-OCFBC **8** has been evaluated in five patients with radiological evidence of metastatic disease and Gleason scores between 7–9 [123]. Normal uptake was predominately in the bladder, kidneys, liver, and heart. The radiopharmaceutical slowly cleared from the blood and was excreted in urine. A total of 32 PET-positive sites were observed with 21 of those sites also seen by either bone scans or CT and were identified as five bone lesions and 16 lymph node lesions. Of the remaining 11 PET-positive sites one was a subcentimeter lymph node and 10 were located on bone and were suggestive of early bone metastases. Of the 10 sites seen by CT and/or bone scans but not visible with ^{18}F-DCFBC, seven were considered to be chronic bone changes or benign fractures. This suggests that ^{18}F-DCFBC may be a more selective agent for detecting bone metastases than is conventional imaging (CT and bone scan). An example of bone lesions detected with ^{18}F-DCFBC is shown in (Fig. 6), which includes a small focus of radioactivity in the left ischium (line arrows in C and D) not seen on the bone scan. An example of a metastatic lymph node visualized with ^{18}F-DCFBC is shown in (Fig. 7).

Normal organ uptake of ^{68}Ga-HBED-CC has been clinically evaluated. Uptake was observed in salivary and lacrimal glands, liver, spleen, intestine and kidneys [141]. Radioactivity in the bladder was not reported. This agent detected a single lesion adjacent to the bladder in a patient with recurrent PCa [142], which was not visible with [^{18}F]fluoro ethylcholine PET/CT. Although, this is only a single case, it demonstrates that radioactivity in the bladder does not restrict the visualization of lesions in the prostate bed using an ^{18}F-labeled PSMA inhibitor of low molecular weight.

BAY1075553 has also been evaluated in patients with proved PCa. The tracer was well tolerated and rapidly cleared from normal organs except for the bladder and kidneys. BAY1075553 detected both primary PCa as well as metastatic lymph nodes and bone lesions, however, degenerative bone lesions also demonstrated intense uptake which could limit the use of this agent for specifically detecting bone metastases [143, 144]. Together these early clinical studies demonstrate the potential clinical utility of PSMA-targeted, low molecular weight PET agents for detecting PCa. Additional clinical studies are needed to validate compounds of this class for a variety of indications.

CONCLUSIONS

A major unmet medical need is a highly specific and sensitive molecular imaging agent or method for staging and monitoring patients with PCa. The ultimate goal of such an agent would actually be predictive, i.e., determining whether a patient’s tumor is indolent vs. aggressive due to the vastly different therapeutic approaches of managing patients with

tumor biology at opposite ends of the spectrum of malignancy. Because PSMA is elevated in aggressive, androgen-insensitive disease, it may serve as an imaging biomarker that reports on tumor biology. For instance, PSMA-targeted imaging agents have been shown in pre-clinical models to report on the activity of androgen signaling and response to taxane therapy [64, 145]. The low molecular weight PSMA inhibitors are particularly promising, with ^{18}F-DCFBC **8**, ^{68}Ga-HBED-CC **15**, and BAY1075553 having proved their mettle in initial clinical studies. Additional clinical studies with these agents and others of this class will be needed to determine the optimal agent and the most appropriate applications for these promising new radiopharmaceuticals.

Acknowledgments

We thank NIH CA134675, CA103175 and CA151838 for financial support.

ABBREVIATIONS

2-PMPA	2-(Phosphonomethyl)pentanedioic acid
AR	Androgen Receptor
CB-TE2A	1,4,8,11-tehaazabicyclo[6.6.2] hexa-decane-4,11-diacetic acid
DCFBC	(S)-2-(3-((R)-1-carboxy-2-((4-fluoro benzyl)thio)ethyl)ureido) pentane dioic acid
DCMC	(S)-2-(3-((R)-1-carboxy-2-(methylthio) ethyl)ureido)pentanedioic acid
DOTA	1,4,7,70-tetraazacyclododecane-N,N’,N”, N”’-tetraacetic acid
DOTA-3A	1,4,7,10-tetraazacyclododecane-N,N’,N”, N”’-triacetic acid
DUPA	2-[3–(1,3-dicarboxypropyl)ureido] pentanedioic acid
FACBC	1-amino-3fluorocyclobutane-1-carboxylic acid
FDG	2-fluoro-2-deoxy-D-glucose
FDHT	16β-fluoro-di-hydrotestosterone
F-Py-TFP	6-fluoronicotinic acid tetrafluorophenyl ester
GI	Gastrointestinal
GCPII	Glutamate carboxypeptidase II
GPI	2-(((3-amino-3-carboxypropyl) (hydroxy) phosphoryl) methyl) pentanedioic acid
HBED	bis-2-hydroxybenryl-ethylene-1,2-N,N’-diacetate
HBED-CC	N,N’-bis[2–hydroxy-5-(carboxy ethyl)-benzyl]ethylenediamine-N,N’-diacetic acid
MR	Magnetic resonance
NAAG	N-acetylaspartyl glutamate

NOTA	1,4,7-triazacyclononane-N,N',N"-triacetic acid
Oxo-DO3A	1-oxa-4,7,10-tetraazacyclododecane 4,7,10-triacetic acid
PAMAM-PEG	Polyamidoamine-polyethylene glycol
PCa	Prostate cancer
PCTA	3,6,9,15-tetraazabicyclo[9.3.1] pentadeca-1(15),11,13-triene-3,6,9-triacetic acid
PET	Positron emission tomography
PKC	Protein kinase C
PSM'	Cytoplasmic PSMA
PSMA	Prostate specific membrane antigen
REC	Recycling endosomal compartment
SCN-Bn-DOTA	S-2-(4-isothiocyanatobenzyl)1,4,7,10-tetraazacyclododecane tetraacetic acid
SFB	N-succinimidyl-4-fluorobenzoate
SPECT	Single photon emission computed tomography
Thr	Threonine
Tyr	Tyrosine

REFERENCES

1. Glunde K, Pathak AP, Bhujwalla ZM. Molecular-functional imaging of cancer: to image and imagine. Trends. Mol. Med. 2007; 13:287–297. [PubMed: 17544849]
2. Higgins LJ, Pomper MG. The evolution of imaging in cancer: current state and future challenges. Semin. Oncol. 2011; 18:3–15. [PubMed: 21362512]
3. Weissleder R, Pittet MJ. Imaging in the era of molecular oncology. Nature. 2008; 452:580–589. [PubMed: 18385732]
4. Jemal A, Siegel R, Ward E, Hao Y, Xu J, Thun MJ. Cancer statistics, 2009. CA. Cancer. J. Clin. 2009; 59:225–249. [PubMed: 19474385]
5. Jadvar H. Molecular imaging of prostate cancer with 18F-fluorodeoxyglucose PET. Nat. Rev. Urol. 2009; 6:317–323. [PubMed: 19434102]
6. Dehdashti F, Picus J, Michalski JM, Dence CS, Siegel BA, Katzenellenbogen JA, Welch MJ. Positron tomographic assessment of androgen receptors in prostatic carcinoma. Eur. J. Nucl. Med. Mol. Imaging. 2005; 32:344–350. [PubMed: 15726353]
7. Larson SM, Monis M, Gunther I, Beattie B, Humm JL, Akhurst TA, Finn RD, Erdi Y, Pentlow K, Dyke J, Squire O, Bornmann W, McCarthy T, Welch M, Scher H. Tumor localization of 16beta-18F-fluoro-5alpha-dihydrotestosterone versus 18F-FDG in patients with progressive, metastatic prostate cancer. J. Nucl. Med. 2004; 45:366–373. [PubMed: 15001675]
8. Kato T, Tsukamoto E, Kuge Y, Takei T, Shiga T, Shinohara N, Katoh C, Nakada K, Tamaki N. Accumulation of [11C]acetate in normal prostate and benign prostatic hyperplasia: comparison with prostate cancer. Eur. J. Nucl. Med. Mol. Imaging. 2002; 29:1492–1495. [PubMed: 12397469]
9. DeGrado TR, Coleman RE, Wang S, Baldwin SW, Orr MD, Robertson CN, Polascik TJ, Price DT. Synthesis and evaluation of 18F-labeled choline as an oncologic tracer for positron emission

tomography: initial findings in prostate cancer. Cancer. Res. 2001; 61:110–117. [PubMed: 11196147]

10. Bauman G, Belhocine T, Kovacs M, Ward A, Beheshti M, Rachinsky I. 18F-fluorocholine for prostate cancer imaging: a systematic review of the literature. Prostate. Cancer. Prostatic. Dis. 2012; 15:45–55. [PubMed: 21844889]
11. Schuster DM, Savir-Baruch B, Nieh PT, Master VA, Halkar RK, Rossi PJ, Lewis MM, Nye JA, Yu W, Bowman FD, Goodman MM. Detection of recurrent prostate carcinoma with anti-1-amino-3-18F-fluorocyclobutane-1-carboxylic acid PET/CT and 111In-capromab pendetide SPECT/CT. Radiology. 2011; 259:852–861. [PubMed: 21493787]
12. Mease RC. Radionuclide based imaging of prostate cancer. Curr. Top Med Chen. 2010; 10:1600–1616.
13. Hong H, Zhang Y, Sun J, Cai W. Positron emission tomography imaging of prostate cancer. Amino. Acids. 2010; 39:11–27. [PubMed: 19946787]
14. Effert PJ, Bares R, Handt S, Wolff JM, Bull U, Jakse G. Metabolic imaging of untreated prostate cancer by positron emission tomography with 18fluorine-labeled deoxyglucose. J. Urol. 1996; 155:994–998. [PubMed: 8583625]
15. Liu IJ, Zafar MB, Lai YH, Segall GM, Terris MK. Fluorodeoryglucose positron emission tomography studies in diagnosis and staging of clinically organ-confined prostate cancer. Urology. 2001; 57:108–111. [PubMed: 11164153]
16. Hofer C, Laubenbacher C, Block T, Breul J, Hartung R, Schwaiger M. Fluorine-18-fluorodeoxyglucose positron emission tomography is useless for the detection of local recurrence after radical prostatectomy. Eur. Urol. 1999; 36:31–35. [PubMed: 10364652]
17. Shreve PD, Grossman HB, Gross MD, Wahl RL. Metastatic prostate cancer: initial findings of PET with 2-deoxy-2-[F-18]fluoro-D-glucose. Radiology. 1996; 199:751–756. [PubMed: 8638000]
18. Richter JA, Rodriguez M, Rioja J, Penuelas I, Marti-Climent J, Garrastachu P, Quincoces G, Zudaire J, Garcia-Velloso MJ. Dual tracer 11C-choline and FDG-PET in the diagnosis of biochemical prostate cancer relapse after radical treatment. Mol. Imaging. Biol. 2010; 12:210–217. [PubMed: 19543774]
19. Schoder H, Herrmann K, Gonen M, Hricak H, Eberhard S, Scardino P, Scher HI, Larson SM. 2-[18F]fluoro-2-deoxyglucose positron emission tomography for the detection of disease in patients with prostate-specific antigen relapse after radical prostatectomy. Clin. Cancer. Res. 2005; 11:4761–4769. [PubMed: 16000572]
20. Schoder H, Larson SM. Positron emission tomography for prostate, bladder, and renal cancer. Semin. Nucl. Med. 2004; 34:274–292. [PubMed: 15493005]
21. Haseman MK, Rosenthal SA, Polascik TJ. Capromab Pendetide imaging of prostate cancer. Cancer. Biother. Radiopharm. 2000; 15:131–140. [PubMed: 10803318]
22. Seo Y, Aparici CM, Cooperberg MR, Konety BR, Hawkins RA. *In vivo* tumor grading of prostate cancer using quantitative 111In-capromab pendetide SPECT/CT. J. Nucl. Med. 2010; 51:31–36. [PubMed: 20008977]
23. Troyer JK, Beckett ML, Wright GL Jr. Location of prostate-specific membrane antigen in the LNCaP prostate carcinoma cell line. Prostate. 1997; 30:232–242. [PubMed: 9111600]
24. Ruggiero A, Holland JP, Hudolin T, Shenker L, Koulova A, Bander NH, Lewis JS, Grimm J. Targeting the internal epitope of prostate-specific membrane antigen with 89Zr-7E11 immuno-PET. J. Nucl. Med. 2011; 52:1608–1615. [PubMed: 21908391]
25. Holland JP, Divilov V, Bander NH, Smith-Jones PM, Larson SM, Lewis JS. 89Zr-DFO-J591 for immunoPET of prostate-specific membrane antigen expression. in. vivo. J. Nucl. Med. 2010; 51:1293–1300.
26. Beattie BJ, Smith-Jones PM, Jhanwar YS, Schoder H, Schmidtlein CR, Morris MJ, Zanzonico P, Squire O, Meirelles GS, Finn R, Namavari M, Cai S, Scher HI, Larson SM, Humm JL. Pharmacokinetic assessment of the uptake of 16beta-18F-fluoro-5alpha-dihydrotestosterone (FDHT) in prostate tumors as measured by PET. J. Nucl. Med. 2010; 51:183–192. [PubMed: 20080885]
27. Oyama N, Akino H, Kanamaru H, Suzuki Y, Muramoto S, Yonekura Y, Sadato N, Yamamoto K, Okada K. 11C-acetate PET imaging of prostate cancer. Nucl. Med. 2002; 43:181–186.

28. de Jong IJ, Pruim J, Elsinga PH, Vaalburg W, Mensink HJ. 11C-choline positron emission tomography for the evaluation after treatment of localized prostate cancer. Eur. Urol. 2003; 44:32–38. discussion 38-9. [PubMed: 12814672]
29. Hara T, Kosaka N, Kishi H. PET imaging of prostate cancer using carbon-11-choline. J Nucl. Med. 1998; 39:990–995. [PubMed: 9627331]
30. Hara T, Kosaka N, Kishi H. Development of (18)F-fluoroethylcholine for cancer imaging with PET: synthesis, biochemistry, and prostate cancer imaging. J. Nucl. Med. 2002; 43:r87–r99.
31. Price DT, Coleman RE, Liao RP, Robertson CN, Polascik TJ, DeGrado TR. Comparison of [18 F]fluorocholine and [18 F]fluorodeoxyglucose for positron emission tomography of androgen dependent and androgen independent prostate cancer. J. Urol. 2002; 68:273–280. [PubMed: 12050555]
32. VallabhajosulaS, KL.; Kothari, PA.; Hamacher, K.; Goldsmith, SJ. Pharmacokinetics and biodishibution of radiolabeled choline in human subjects: comparison of [11C]choline and [18F]choline. Journal of Labelled Compounds and Radiopharmaceuticals; 16th International Symposium on Radiopharmaceutical Chemistry; Iowa City, Iowa. 2005. p. S281
33. Sutinen E, Nurmi M, Roivainen A, Varpula M, Tolvanen T, Lehikoinen P, Minn H. Kinetics of [(11)C]choline uptake in prostate cancer: a PET study. Eur. J. Nucl. Med. MoL Imaging. 2004; 31:317–324. [PubMed: 14628097]
34. Connors TA, Elson LA, Haddow A, Ross WC. The pharmacology and tumour growth inhibitory activity of 1-aminocyclopentane-1-carboxylic acid and related compounds. Bio-chem. Pharmacol. 1960; 5:108–129.
35. Okudaira H, Shikano N, Nishii R, Miyagi T, Yoshimoto M, Kobayashi M, Ohe K, Nakanishi T, Tamai I, Namiki M, Kawai K. Putative transport mechanism and intracellular fate of trans-1-amino-3-18F-fluorocyclobutanecarboxylic acid in human prostate cancer. J Nucl. Med. 2011; 52:822–829. [PubMed: 21536930]
36. Asano Y, Inoue Y, Ikeda Y, Kikuchi K, Hara T, Taguchi C, Tokushige T, Maruo H, Takeda T, Nakamura T, Fujita T, Kumagai Y, Hayakawa K. Phase I clinical study of NMK36: a new PET tracer with the synthetic amino acid analogue anti-[18F]FACBC. Ann. Nucl. Med. 2011; 25:414–418. [PubMed: 21409348]
37. Nye JA, Schuster DM, Yu W, Camp VM, Goodman MM, Votaw JR. Biodistribution and radiation dosimetry of the synthetic nonmetabolized amino acid analogue anti-18F-FACBC in humans. J. Nucl. Med. 2007; 48:1017–1020. [PubMed: 17504867]
38. Schuster DM, Votaw JR, Nieh PT, Yu W, Nye JA, Master V, Bowman FD, Issa MM, Goodman MM. Initial experience with the radiotracer anti-1-amino-3-18F-fluorocyclobutane-1-carboxylic acid with PET/CT in prostate carcinoma. J. Nucl. Med. 2007; 48:56–63. [PubMed: 17204699]
39. Chang SS, Reuter VE, Heston WD, Gaudin PB. Comparison of anti-prostate-specific membrane antigen antibodies and other immunomarkers in metastatic prostate carcinoma. Urology. 2001; 57:1179–1183. [PubMed: 11377343]
40. Wright GL Jr, Grob BM, Haley C, Grossman K, Newhall K, Petrylak D, Troyer J, Konchuba A, Schellhammer PF, Moriarty R. Upregulation of prostate-specific membrane antigen after androgen-deprivation therapy. Urology. 1996; 48:326–334. [PubMed: 8753752]
41. Perner S, Hofer MD, Kim R, Shah RB, Li H, Moller P, Hautmann RE, Gschwend JE, Kuefer R, Rubin MA. Prostate-specific membrane antigen expression as a predictor of prostate cancer progression. Hum. Pathol. 2007; 38:696–701. [PubMed: 17320151]
42. Antunes AA, Leite KR, Sousa-Canavez JM, Camara-Lopes LH, Srougi M. The role of prostate specific membrane antigen and pepsinogen C tissue expression as an adjunctive method to prostate cancer diagnosis. J. Urol. 2009; 181:594–600. [PubMed: 19084862]
43. Ghosh A, Heston WD. Tumor target prostate specific membrane antigen (PSMA) and its regulation in prostate cancer. J. Cell. Bio-chem. 2004; 91:528–539.
44. Mhawech-Fauceglia P, Zhang S, Terracciano L, Sauter G, Chadhuri A, Herrmann FR, Penetrante R. Prostate-specific membrane antigen (PSMA) protein expression in normal and neo-plastic tissues and its sensitivity and specificity in prostate adeno-carcinoma: an immunohistochemical study using mutiple tumour tissue microarray technique. Histopathology. 2007; 50:472–483. [PubMed: 17448023]

45. Rovenska M, Hlouchova K, Sacha P, Mlcochova P, Horak V, Zamecnik J, Barinka C, Konvalinka J. Tissue expression and enzymologic characterization of human prostate specific membrane antigen and its rat and pig orthologs. Prostate. 2008; 68:171–182. [PubMed: 18076021]

46. Silver DA, Pellicer L, Fair WR, Heston WD, Cordon-Cardo C. Prostate-specific membrane antigen expression in normal and malignant human tissues. Clin. Cancer. Res. 1997; 3:81–85. [PubMed: 9815541]

47. Samplaski MK, Heston W, Elson P, Magi-Galtuzzi C, Hansel DE. Folate hydrolase (prostate-specific membrane [corrected] antigen) 1 expression in bladder cancer subtypes and associated tumor neovasculature. Mod. Pathol. 2011; 24:1521–1529. [PubMed: 21725290]

48. Wang W, Tavora F, Sharma R, Eisenberger M, Netto GJ. PSMA expression in Schwannoma: a potential clinical mimicker of metastatic prostate carcinoma. Urol. Oncol. 2009; 27:525–528. [PubMed: 18534872]

49. Chang SS, O'Keefe DS, Bacich DJ, Reuter VE, Heston WD, Gaudin PB. Prostate-specific membrane antigen is produced in tumor-associated neovasculature. Clin. Cancer. Res. 1999; 5:2674–2681. [PubMed: 10537328]

50. Chang SS, Reuter VE, Heston WD, Bander NH, Grauer LS, Gaudin PB. Five different anti-prostate-specific membrane antigen (PSMA) antibodies confirm PSMA expression in tumor-associated neovasculature. Cancer. Res. 1999; 59:3192–3198. [PubMed: 10397265]

51. Chang SS, Reuter VE, Heston WD, Gaudin PB. Metastatic renal cell carcinoma neovasculature expresses prostate-specific membrane antigen. Urology. 2001; 57:801–805. [PubMed: 11306418]

52. Haffner MC, Kronberger IE, Ross JS, Sheehan CE, Zitt M, Muhlmann G, Ofner D, Zelger B, Ensinger C, Yang XJ, Geley S, Margreiter R, Bander NH. Prostate-specific membrane antigen expression in the neovasculature of gastric and colorectal cancers. Hum. Pathol. 2009; 40:1754–1761. [PubMed: 19716160]

53. Carter RE, Feldman AR, Coyle JT. Prostate-specific membrane antigen is a hydrolase with substrate and pharmacologic characteristics of a neuropeptidase. Proc. Natl. Acad. Sci. U. S. A. 1996; 93:749–753. [PubMed: 8570628]

54. Robinson MB, Blakely RD, Couto R, Coyle JT. Hydrolysis of the brain dipeptide N-acetyl-L-aspartyl-L-glutamate. Identification and characterization of a novel N-acetylated alpha-linked acidic dipeptidase activity from rat brain. J. Biol. Chem. 1981; 262:14498–14506. [PubMed: 3667587]

55. Halsted CH. The intestinal absorption of folates. Am. J. Clin. Nutr. 1979; 32:846–855. [PubMed: 34996]

56. Sirotnak FM, Tolner B. Carrier-mediated membrane transport of folates in mammalian cells. Annu. Rev. Nutr. 1999; 19:91–122. [PubMed: 10448518]

57. DeMarzo AM, Nelson WG, Isaacs WB, Epstein JI. Pathological and molecular aspects of prostate cancer. Lancet. 2003; 361:955–964. [PubMed: 12648986]

58. Grauer LS, Lawler KD, Marignac JL, Kumar A, Goel AS, Wolfert RL. Identification, purification, and subcellular localization of prostate-specific membrane antigen PSM protein in the LNCaP prostatic carcinoma cell line. Cancer. Res. 1998; 58:4787–4789. [PubMed: 9809977]

59. Heston WD. Characterization and glutamyl preferring carboxypeptidase function of prostate specific membrane antigen: a novel folate hydrolase. Urology. 1997; 49:104–112. [PubMed: 9123729]

60. Su SL, Huang IP, Fair WR, Powell CT, Heston WD. Alternatively spliced variants of prostate-specific membrane antigen RNA: ratio of expression as a potential measurement of progression. Cancer. Res. 1995; 55:1441–1443. [PubMed: 7882349]

61. Wright GL Jr, Haley C, Beckett ML, Schellhammer PF. Expression of prostate-specific membrane antigen in normal, benign, and malignant prostate tissues. Urol. Oncol. 1995; 1:18–28. [PubMed: 21224086]

62. Birtle AJ, Freeman A, Masters JR, Payne HA, Harland SJ. Tumour markers for managing men who present with metastatic prostate cancer and serum prostate-specific antigen levels of <10 ng/mL. BJU. Int. 2005; 96:303–307. [PubMed: 16042718]

63. Denmeade SR, Sokoll LJ, Dalrymple S, Rosen DM, Gady AM, Bruzek D, Ricklis RM, Isaacs JT. Dissociation between androgen responsiveness for malignant growth vs. expression of prostate

specific differentiation markers PSA, hK2, and PSMA in human prostate cancer models. Proslate. 2003; 54:249–257.

64. Evans MJ, Smith-Jones PM, Wongvipat J, Navarro V, Kim S, Bander NH, Larson SM, Sawyers CL. Noninvasive measurement of androgen receptor signaling with a positron-emitting radiopharmaceutical that targets prostate-specific membrane antigen. Proc. Natl. Acad. Sci. U S A. 2011; 108:9578–9582. [PubMed: 21606347]
65. Lambert LA, Mitchell SL. Molecular evolution of the transferrin receptor/glutamate carboxypeptidase II family. J. Mol. Evol. 2007; 64:113–128. [PubMed: 17160644]
66. Mahadevan D, Saldanha JW. The extracellular regions of PSMA and the transferrin receptor contain an aminopeptidase domain: implications for drug design. Protein. Sci. 1999; 8:2546–2549. [PubMed: 10595564]
67. Dautry-Varsat A. Receptor-mediated endocytosis: the intracellular journey of transferrin and its receptor. Biochimie. 1986; 68:375–381. [PubMed: 2874839]
68. Schulke N, Varlamova OA, Donovan GP, Ma D, Gardner JP, Morrissey DM, Arrigale RR, Zhan C, Chodera AJ, Surowitz KG, Maddon PJ, Heston WD, Olson WC. The homodimer of prostate-specific membrane antigen is a functional target for cancer therapy. Proc. Natl. Acad. Sci. U S A. 2003; 100:12590–12595. [PubMed: 14583590]
69. Carrasquillo J. Imaging and dosimetry determinations using radio-labeled antibodies. Cancer. Treat. Res. 1993; 68:65–97. [PubMed: 8105853]
70. Commandeur LC, Parsons JR. Degradation of halogenated aromatic compounds. Biodegradation. 1990; 1:207–220. [PubMed: 1368148]
71. Grant BD, Donaldson JG. Pathways and mechanisms of endocytic recycling. Nat. Rev. Mol. Cell. Biol. 2009; 10:597–608. [PubMed: 19696797]
72. Yao V, Bacich DJ. Prostate specific membrane antigen (PSMA) expression gives prostate cancer cells a growth advantage in a physiologically relevant folate environment *in vitro*. Prostate. 2006; 66:867–875. [PubMed: 16496414]
73. Yao V, Berkman CE, Choi JK, O'Keefe DS, Bacich DJ. Expression of prostate-specific membrane antigen (PSMA), increases cell folate uptake and proliferation and suggests a novel role for PSMA in the uptake of the non-polyglutamated folate, folic acid. Prostate. 2010; 70:305–316. [PubMed: 19830782]
74. Yao V, Parwani A, Maier C, Heston WD, Bacich DJ. Moderate expression of prostate-specific membrane antigen, a tissue differentiation antigen and folate hydrolase, facilitates prostate carcinogenesis. Cancer. Res. 2008; 68:9070–9077. [PubMed: 18974153]
75. Vallabhajosula S, Kuji I, Hamacher KA, Konishi S, Kostakoglu L, Kothari PA, Milowski ML, Nanus DM, Bander NH, Goldsmith SJ. Pharmacokinetics and biodistribution of 111In- and 177Lu-labeled J591 antibody specific for prostate-specific membrane antigen: prediction of 90Y-J591 radiation dosimetry based on 111In or 177Lu? J. Nucl. Med. 2005; 46:634–641. [PubMed: 15809486]
76. Bander NH, Trabulsi EJ, Kostakoglu L, Yao D, Vallabhajosula S, Smith-Jones P, Joyce MA, Milowsky M, Nanus DM, Goldsmith SJ. Targeting metastatic prostate cancer with radiolabeled monoclonal antibody J591 to the extracellular domain of prostate specific membrane antigen. J. Urol. 2003; 170:1717–1721. [PubMed: 14532761]
77. Bander NH, Milowsky MI, Nanus DM, Kostakoglu L, Vallabhajosula S, Goldsmith SJ. Phase I trial of 177lutetium-labeled *J591*, a monoclonal antibody to prostate-specific membrane antigen, in patients with androgen-independent prostate cancer. J. Clin. Oncol. 2005; 23:4591–4601. [PubMed: 15837970]
78. Elsasser-Beile U, Wolf P, Gierschner D, Buhler P, Schultze-Seemann W, Wetterauer U. A new generation of monoclonal and recombinant antibodies against cell-adherent prostate specific membrane antigen for diagnostic and therapeutic targeting of prostate cancer. Prostate. 2006; 66:1359–1370. [PubMed: 16894535]
79. Alt K, Wiehr S, Ehrlichmann W, Reischl G, Wolf P, Pichler BJ, Elsasser-Beile U, Buhler P. High-resolution animal PET imaging of prostate cancer xenografts with three different 64Cu-labeled antibodies against native cell-adherent PSMA. Prostate. 2010; 70:1413–1421. [PubMed: 20687214]

80. Viola-Villegas, N.; Evans, H.; Bartlett, D.; Wu, A.; Lewis, J. Pre-clinical development of Zr-89 labeled anti-PSMA minibody and cys-diabody. Abstracts of the Society of Nuclear Medicine Annual Meeting; June. 9-13, 2012; Miami. Beach, Florida.
81. Cerchia L, Giangrande PH, McNamara JO, de Franciscis V. Cell-specific aptamers for targeted therapies. Methods. Mol. Biol. 2009; 535:59–78. [PubMed: 19377980]
82. Lupold SE, Hicke BJ, Lin Y, Coffey DS. Identification and characterization of nuclease-stabilized RNA molecules that bind human prostate cancer cells via the prostate-specific membrane antigen. Cancer. Res. 2002; 62:4029–4033. [PubMed: 12124337]
83. Bagalkot V, Farokhzad OC, Langer R, Jon S. An aptamer-doxorubicin physical conjugate as a novel targeted drug-delivery platform. Angew. Chem. Int. Ed Engl. 2006; 45:8149–8152. [PubMed: 17099918]
84. Dassie JP, Liu XY, Thomas GS, Whitaker RM, Thiel KW, Stockdale KR, Meyerholz DK, McCaffrey AP, McNamara JO 2nd, Giangrande PH. Systemic administration of optimized aptamer-siRNA chimeras promotes regression of PSMA-expressing tumors. Nat. Biotechnol. 2009; 27:839–849. [PubMed: 19701187]
85. Kim D, Jeong YY, Jon S. A drug-loaded aptamer-gold nanoparticle bioconjugate for combined CT imaging and therapy of prostate cancer. ACS. Nano. 2010; 4:3689–3696. [PubMed: 20550178]
86. Ni X, Zhang Y, Ribas J, Chowdhury WH, Castanares M, Zhang Z, Laiho M, DeWeese TL, Lupold SE. Prostate-targeted radiosensitization via aptamer-shRNA chimeras in human tumor xenografts. J. Clin. Invest. 2011; 121:2383–2390. [PubMed: 21555850]
87. Chu TC, Marks JW 3rd, Lavery LA, Faulkner S, Rosenblum MG, Ellington AD, Levy M. Aptamer:toxin conjugates that specifically target prostate tumor cells. Cancer. Res. 2006; 66:5989–5992. [PubMed: 16778167]
88. Dhar S, Gu FX, Langer R, Farokhzad OC, Lippard SJ. Targeted delivery of cisplatin to prostate cancer cells by aptamer functionalized Pt(IV) prodrug-PLGA-PEG nanoparticles. Proc. Natl. Acad. Sci. U S A. 2008; 105:17356–17361. [PubMed: 18978032]
89. Farokhzad OC, Cheng J, Teply BA, Sherifi I, Jon S, Kantoff PW, Richie JP, Langer R. Targeted nanoparticle-aptamer bioconjugates for cancer chemotherapy *in vivo*. Proc. Natl. Acad. Sci. U S A. 2006; 103:6315–6320. [PubMed: 16606824]
90. Farokhzad OC, Jon S, Khademhosseini A, Tran TN, Lavan DA, Langer R. Nanoparticle-aptamer bioconjugates: a new approach for targeting prostate cancer cells. Cancer. Res. 2004; 64:7668–7672. [PubMed: 15520166]
91. Wang AZ, Bagalkot V, Vasilliou CC, Gu F, Alexis F, Zhang L, Shaikh M, Yuet K, Cima MJ, Langer R, Kantoff PW, Bander NH, Jon S, Farokhzad OC. Superparamagnetic iron oxide nanoparticle-aptamer bioconjugates for combined prostate cancer imaging and therapy. ChemMedChem. 2008; 3:1311–1315. [PubMed: 18613203]
92. Zhang L, Radovic-Moreno AF, Alexis F, Gu FX, Basto PA, Bagalkot V, Jon S, Langer RS, Farokhzad OC. Co-delivery of hydrophobic and hydrophilic drugs from nanoparticle-aptamer bioconjugtes. ChemMedChem. 2007; 2:1268–1271. [PubMed: 17600796]
93. Bagalkot Y, Zhang L, Levy-Nissenbaum E, Jon S, Kantoff PW, Langer R, Farokhzad OC. Quantum dot-aptamer conjugates for synchronous cancer imaging, therapy, and sensing of drug delivery based on bi-fluorescence resonance energy transfer. Nano. Lett. 2007; 7:3065–3070. [PubMed: 17854227]
94. Wu X, Ding B, Gao J, Wang H, Fan W, Wang X, Zhang W, Ye L, Zhang M, Ding X, Liu J, Zhu Q, Gao S. Second-generation aptamer-conjugated PSMA-targeted delivery system for prostate cancer therapy. Int. J. Nanonedicine. 2011; 6:1747–1756.
95. Rockey WM, Huang L, Kloepping KC, Baumhover NJ, Giangrande PH, Schultz MK. Synthesis and radiolabeling of chelator-RNA aptamer bioconjugates with copper-64 for targeted molecular imaging. Bioorg. Med. Chem. 2011; 19:4080–4090. [PubMed: 21658962]
96. Barinka C, Byun Y, Dusich CL, Banerjee SR, Chen Y, Castanares M, Kozikowski AP, Mease RC, Pomper MG, Lubkowski J. Interactions between human glutamate carboxypeptidase II and urea-based inhibitors: structural characterization. J Med. Chem. 2008; 51:7737–7743. [PubMed: 19053759]

97. Barinka C, Rovenska M, Mlcochova P, Hlouchova K, Plechanovova A, Majer P, Tsukamoto T, Slusher BS, Konvalinka J, Lubkowski J. Structural insight into the pharmacophore pocket of human glutamate carboxypeptidase II. J. Med. Chem. 2007; 50:3267–3273. [PubMed: 17567119]

98. Barinka C, Starkova J, Konvalinka J, Lubkowski J. A high-resolution structure of ligand-free human glutamate carboxypeptidase II. Acta. Crystallogr. Sect. F. Struct. Biol. Cryst. Commun. 2007; 63:150–153.

99. Davis MI, Bennett MJ, Thomas LM, Bjorkman PJ. Crystal structure of prostate-specific membrane antigen, a tumor marker and peptidase. Proc. Natl. Acad. Sci. U. S. A. 2005; 102:5981–5986. [PubMed: 15837926]

100. Mesters JR, Barinka C, Li W, Tsukamoto T, Majer P, Slusher BS, Konvalinka J, Hilgenfeld R. Structure of glutamate carboxypeptidase II, a drug target in neuronal damage and prostate cancer. EMBO. J. 2006; 25:1375–1384. [PubMed: 16467855]

101. Mesters JR, Henning K, Hilgenfeld R. Human glutamate carboxypeptidase II inhibition: structures of GCPII in complex with two potent inhibitors, quisqualate and 2-PMPA. Acta. Crystallogr. D. Biol. Crystallogr. 2007; 63:508–513. [PubMed: 17372356]

102. Wang H, Byun Y, Barinka C, Pullambhatla M, Bhang HE, Fox JJ, Lubkowski J, Mease RC, Pomper MG. Bioisosterism of urea-based GCPII inhibitors: Synthesis and structure-activity relationship studies. Bioorg. Med. Chem. Lett. 2010; 20:392–397. [PubMed: 19897367]

103. Byun, Y.; Mease, RC.; Lupold, SE.; Pomper, MG. Recent Development of Diagnostic and Therapeutic Agents Targeting Glutamate Carboxylpeptidase II. (GCPII). John Wiley & Sons: 2009. Chapter 36.

104. Zhou J, Neale JH, Pomper MG, Kozikowski AP. NAAG peptidase inhibitors and their potential for diagnosis and therapy. Nat. Rev. Drug. Discov. 2005; 4:1015–1026. [PubMed: 16341066]

105. Slusher BS, Vomov JJ, Thomas AG, Hum PD, Harukuni I, Bhardwaj A, Traystman RJ, Robinson MB, Britton P, Lu XC, Tortella FC, Wozniak KM, Yudkoff M, Potter BM, Jackson PF. Selective inhibition of NAALADase, which converts NAAG to glutamate, reduces ischemic brain injury. Nat. Med. 1999; 5:1396–1402. [PubMed: 10581082]

106. Jackson PF, Cole DC, Slusher BS, Stetz SL, Ross LE, Donzanti BA, Trainor DA. Design, synthesis, and biological activity of a potent inhibitor of the neuropeptidase N-acetylated alpha-linked acidic dipeptidase. J. Med. Chem. 1996; 39:619–622. [PubMed: 8558536]

107. Majer P, Jackson PF, Delahanty G, Grella BS, Ko YS, Li W, Liu Q, Maclin KM, Polakova J, Shaffer KA, Stoermer D, Vitharana D, Wang EY, Zakrzewski A, Rojas C, Slusher BS, Wozniak KM, Burak E, Limsakun T, Tsukamoto T. Synthesis and biological evaluation of thiol-based inhibitors of glutamate carborypeptidase II: discovery of an orally active GCP II inhibitor. J. Med. Chem. 2003; 46:1989–1996. [PubMed: 12723961]

108. Anderson MO, Wu LY, Santiago NM, Moser JM, Rowley JA, Bolstad ES, Berkman CE. Substrate specificity of prostate-specific membrane antigen. Bioorg. Med. Chen. 2007; 15:6678–6686.

109. Liu T, Wu LY, Kazak M, Berkman CE. Cell-Surface labeling and internalization by a fluorescent inhibitor of prostate-specific membrane antigen. Prostate. 2008; 68:955–964. [PubMed: 18361407]

110. Maung J, Mallari JP, Girtsman TA, Wu LY, Rowley JA, Santiago NM, Brunelle AN, Berkman CE. Probing for a hydrophobic a binding register in prostate-specific membrane antigen with phenylalkylphosphonamidates. Bioorg. Med. Chem. 2004; 12:4969–4979. [PubMed: 15336276]

111. Kozikowski AP, Nan F, Conti P, Zhang J, Ramadan E, Bzdega T, Wroblewska B, Neale JH, Pshenichkin S, Wroblewski JT. Design of remarkably simple, yet potent urea-based inhibitors of glutamate carboxypeptidase II (NAALADase). J. Med. Chem. 2001; 44:298–301. [PubMed: 11462970]

112. Kozikowski AP, Zhang J, Nan F, Petukhov PA, Grajkowska E, Wroblewski JT, Yamamoto T, Bzdega T, Wroblewska B, Neale JH. Synthesis of urea-based inhibitors as active site probes of glutamate carboxypeptidase II: efficacy as analgesic agents. J. Med. Chem. 2004; 47:1729–1738. [PubMed: 15027864]

113. Liu T, Wu LY, Hopkins MR, Choi JK, Berkman CE. A targeted low molecular weight near-infrared fluorescent probe for prostate cancer. Bioorg. Med. Chem. Lett. 2010; 20:7124–7126. [PubMed: 20947349]

114. Nedrow-Byers JR, Jabbes M, Jewett C, Ganguly T, He H, Liu T, Benny P, Bryan JN, Berkman CE. A phosphorami-date-based prostate-specific membrane antigen-targeted SPECT agent. Prostate. 2012; 72:904–912. [PubMed: 22670265]

115. Nedrow-Byers JR, Moore AL, Ganguly T, Hopkins MR, Fulton MD, Benny PD, Berkman CE. PSMA-targeted SPECT agents: Mode of binding effect on *in vitro* performance. Prostate. 2012

116. Hao, GKA.; Gore, C.; Dobin, T.; Singh, A.; Oz, O.; Hsieh, J-T.; Sun, X. PET signal amplification via bifunctional chelator scaffold for the prostate specific membrane antigen (PSMA) detection. Abstracts of the Society of Nucleor Medicine Annual Meeting; June, 9-13, 2012; Miami Beach, Florida.

117. Graham, K.; Kettschau, G.; Gromov, A.; Friebe, M.; Gekeler, V.; Dinkelborg, L. [18F]-labeled PET tracer BAY1075553, small molecule inhibitor of PSMA for molecular Imaging of prostate cancer; World Molecular Imaging Conference; Sept. 7-10; San Diego, California. 2011. p. P235

118. Pomper MG, Musachio JL, Zhang J, Scheffel U, Zhou Y, Hilton J, Maini A, Dannals RF, Wong DF, Kozikowski AP. 11C-MCG: synthesis, uptake selectivity, and primate PET of a probe for glutamate carboxypeptidase II (NAALADase). Mol Imaging. 2002; 1:96–101. [PubMed: 12920850]

119. Foss CA, Mease RC, Fan H, Wang Y, Ravert HT, Dannals RF, Olszewski RT, Heston WD, Kozikowski AP, Pomper MG. Radiolabeled small-molecule ligands for prostate-specific membrane antigen: *in vivo* imaging in experimental models of prostate cancer. Clin. Cancer. Res. 2005; 11:4022–4028. [PubMed: 15930336]

120. Ravert HT, Madar I, Dannals RF. Radiosynthesis of 3-[^{18}F]fluoropropyl and 4-[^{18}F]fluorobenzyl triarylphosphoniums ions. J. Label. Compd. Radiopharm. 2004; 47:469–476.

121. Mease RC, Dusich CL, Foss CA, Ravert HT, Dannals RF, Seidel J, Prideaux A, Fox JJ, Sgouros G, Kozikowski AP, Pomper MG. N-[N-(S)-1,3-Dicarboxypropyl]carbamoyl]-4-[18F]fluorobenzyl-L-cysteine, [18F]DCFBC: a new imaging probe for prostate cancer. Clin. Cancer. Res. 2008; 14:3036–3043. [PubMed: 18483369]

122. Holt DP, Ravert HT, Mathews WB, Horti A, Mease R, Dannals RF. A semi-automated microwave chemistry system for complete radiosynthesis, purification, and formulation of F-18 radiotracers. J. Label. Compd. Radiopharm. 2011; 54:S426.

123. Cho SY, Gage KL, Mease RC, Senthamizhchelvan S, Holt DP, Kwanisai-Jeffrey A, Endres CJ, Dannals RF, Sgouros G, Lodge M, Eisenberger MA, Rodriguezx R, Carducci MA, Rojas C, Slusher BS, Kozikowski AP, Pomper MG. Biodistribution, tumor detection and Radiation dosimetry of ^{18}F-DCFBC, a low molecular weight inhibitor of PSMA, in patients with metastatic prostate cancer. J. Nucl. Med. 2012; 53:1883–1891. [PubMed: 23203246]

124. Chen Y, Foss CA, Byun Y, Nimmagadda S, Pullambhatla M, Fox JJ, Castanares M, Lupold SE, Babich JW, Mease RC, Pomper MG. Radiohalogenated prostate-specific membrane antigen (PSMA)-based ureas as imaging agents for prostate cancer. J. Med. Chem. 2008; 51:7933–7943. [PubMed: 19053825]

125. Olberg DE, Arukwe JM, Grace D, Hjelstuen OK, Solbakken M, Kindberg GM, Cuthbertson A. One step radiosynthesis of 6-[(18)F]fluoronicotinic acid 2,3,5,6-tetrafluorophenyl ester ((18)F]F-Py-TFP): a new prosthetic group for efficient labeling of biomolecules with fluorine-18. J. Med. Chem. 2010; 53:1732–1740. [PubMed: 20088512]

126. Chen Y, Pullambhatla M, Foss CA, Byun Y, Nimmagadda S, Senthamizhchelvan S, Sgouros G, Mease RC, Pomper MG. 2-(3-{1-Carboxy-5-[(6-[18F]fluoro-pyridine-3-carbonyl)-amino]-pentyl}-ureido)-pen tanedioic acid, [18F]DCFPyL, a PSMA-based PET imaging agent for prostate cancer. Clin. Cancer. Res. 2011; 17:7645–7653. [PubMed: 22042970]

127. Kothari, P.; Vallabhajosula, S.; Schoendorf, M.; Lu, G.; Zimmerman, C.; Hillier, S.; Maresca, K.; Eckelman, W.; Joyal, J.; Babich, J. 18F-labeled small molecule inhibitors of prostate specific membrane antigen (PSMA) for PET imaging of prostate cancer. Abstracts of the Society of Nuclear Medicine Annual Meeting; June 9-13, 2012; Miami Beach, Florida.

128. Banerjee SR, Pullambhatla M, Byun Y, Nimmagadda S, Green G, Fox JJ, Horti A, Mease RC, Pomper MC. 68Ga-labeled inhibitors of prostate-specific membrane antigen (PSMA) for imaging prostate cancer. J. Med. Chem. 2010; 53:5333–5341. [PubMed: 20568777]

129. Banerjee SR, Foss CA, Castanares M, Mease RC, Byun Y, Fox JJ, Hilton J, Lupold SE, Kozikowski AP, Pomper MG. Synthesis and evaluation of technetium-99m- and rhenium-labeled inhibitors of the prostate-specific membrane antigen (PSMA). J. Med. Chem. 2008; 51:4504–4517. [PubMed: 18637669]

130. Kularatne SA, Zhou Z, Yang J, Post CB, Low PS. Design, synthesis, and preclinical evaluation of prostate-specific membrane antigen targeted (99m)Tc-radioimaging agents. Mol. Pharm. 2009; 6:790–800. [PubMed: 19361232]

131. Roesch F, Riss PJ. The renaissance of the (6)(8)Ge/(6)(8)Ga radionuclide generator initiates new developments in (6)(8)Ga radio-pharmaceutical chemistry. Curr. Top. Med. Chem. 2010; 10:1633–1668. [PubMed: 20583984]

132. Eder M, Schafer M, Bauder-Wust U, Hull WE, Wangler C, Mier W, Haberkom U, Eisenhut M. 68Ga-complex lipophilicity and the targeting property of a urea-based PSMA inhibitor for PET imaging. Bioconjug. Chem. 2012; 23:688–697. [PubMed: 22369515]

133. Schafer M, Bauder-Wust U, Leotta K, Zoller F, Mier W, Haberkorn U, Eisenhut M, Eder M. A dimerized urea-based inhibitor of the prostate-specific membrane antigen for 68Ga-PET imaging of prostate cancer. EJNMMI Res. 2012; 2:23. [PubMed: 22673157]

134. Banerjee SR, Pullambhatla M, Byun Y, Foss C, Nimmagadda S, Ferdani R, Anderson CJ, Mease RC, Pomper MG. 64Cu-labeled inhibitors of prostate specific membrane antigen for PET imaging of prostate cancer. J. Label. Compd. Radiopharm. 2011; 54:S369.

135. Banerjee SR, Pullambhatla M, Byun Y, Nimmagadda S, Baidoo K, Brechbiel MW, Mease RC, Pomper MG. Preclinical evaluation of 86Y-labeled inhibitors of prostate specific membrane antigen. J. Label. Compd. Radiopharm. 2011; 54:S65.

136. Chen Y, Dhara S, Banerjee SR, Byun Y, Pullambhatla M, Mease RC, Pomper MG. A low molecular weight PSMA-based fluorescent imaging agent for cancer. Biochem Biophys. Res. Commun. 2009; 390:624–629. [PubMed: 19818734]

137. Chandran SS, Banerjee SR, Mease RC, Pomper MG, Denmeade SR. Characterization of a targeted nanoparticle functionalized with a urea-based inhibitor of prostate-specific membrane antigen (PSMA). Cancer. Biol. Ther. 2008; 7:974–982. [PubMed: 18698158]

138. Hrkach J, Von Hoff D, Mukkaram Ali M, Andrianova E, Auer J, Campbell T, De Witt D, Figa M, Figueiredo M, Horhota A, Low S, McDonnell K, Peeke E, Retnarajan B, Sabris A, Schnipper E, Song JJ, Song YH, Summa J, Tompsett D, Troiano G, Van Geen Hoven T, Wright J, LoRusso P, Kantoff PW, Bander NH, Sweeney C, Farokhzad OC, Langer R, Zale S. Preclinical development and clinical translation of a PSMA-targeted docetaxel nanoparticle with a differentiated pharmacological profile. Sci. Transl. Med. 2012; 4 128ra39.

139. Kularatne SA, Wang K, Santhapuram HK, Low PS. Prostate-specific membrane antigen targeted imaging and therapy of prostate cancer using a PSMA inhibitor as a homing ligand. Mol. Pharm. 2009; 6:780–789. [PubMed: 19361233]

140. Malik, N.; Zlatopolskiy, B.; Solbach, C.; Machulla, H-J.; Reske, S. One pot radiosynthesis of a new PSMA ligand [A118F]NOTA-DUPA-Pep. Abstracts of the Annual Meeting of the Society of Nyclear Medicine; June. 9-13; Miami. Beach, Florida. 2012.

141. Afshar-Oromieh, A.; Zechmann, C.; Eder, M.; Eisenhut, M.; Haberkorn, U. [68Ga]Gallium labelled PSMA ligand as new PET-tracer for the diagnosis of prostate cancer: Normal uptake of healthy tissue. Abstracts of the Annual Meeting of the Society of Nyclear Medicine; June. 9-13, 2012; Miami. Beach, Florida.

142. Afshar-Oromieh A, Haberkom U, Eder M, Eisenhut M, Zechmann CM. [68Ga]Gallium-labelled PSMA ligand as superior PET tracer for the diagnosis of prostate cancer: comparison with 18F-FECH. Eur. J. Nucl. Med. Mol. Imaging. 2012; 39:1085–1086. [PubMed: 22310854]

143. Langsteger W, Kunit T, Haim S, Nader M, Valencia R, Lesche R, Sega W, Piert M, Loidl W, Beheshti M. BAY 1075553 PET/CT in the assessment of prostate cancer: Safety, tolerability and biodistribution - Phase I first in human study results. J. Nucl. Med. 2012; 53:1125.

144. Beheshti M, Langsteger W, Sommerhuber A, Steinmair M, Wolf I, Valencia R, Lesche R, Nader M, Piert M, Loidl W. BAY 1075553 in staging and restaging of prostate cancer patients - Phase I study and comparison to 18F-FCH. J. Nucl. Med. 2012; 53:272.

145. Hillier SM, Kem AM, Maresca KP, Marquis JC, Eckelman WC, Joyal JL, Babich JW. 1231-MIP-1072, a small-molecule inhibitor of prostate-specific membrane antigen, is effective at monitoring tumor response to taxane therapy. J. Nucl. Med. 2011; 52:1082–1093.

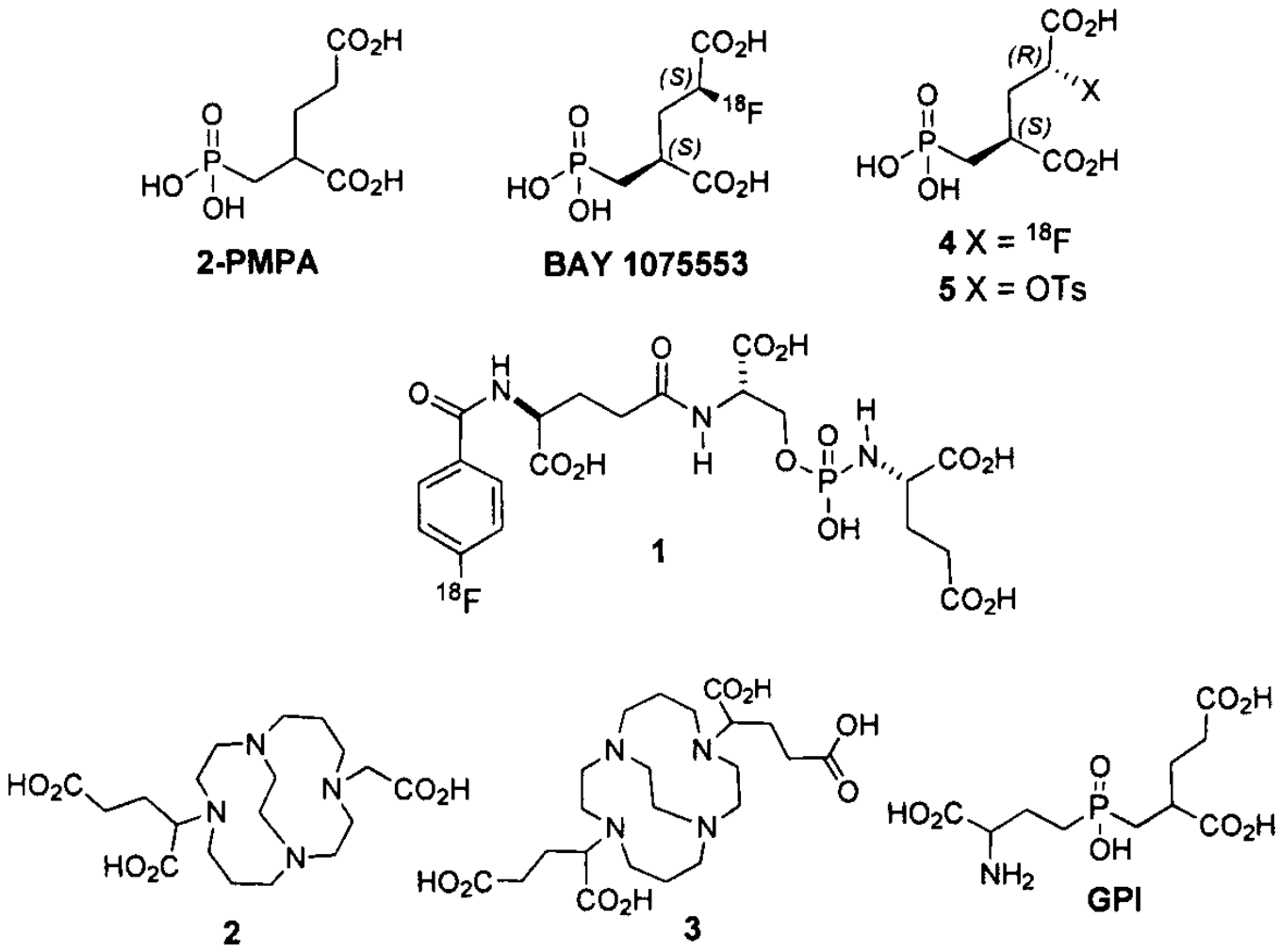

Fig. 1.
PET agents derived from 2-PMPA.

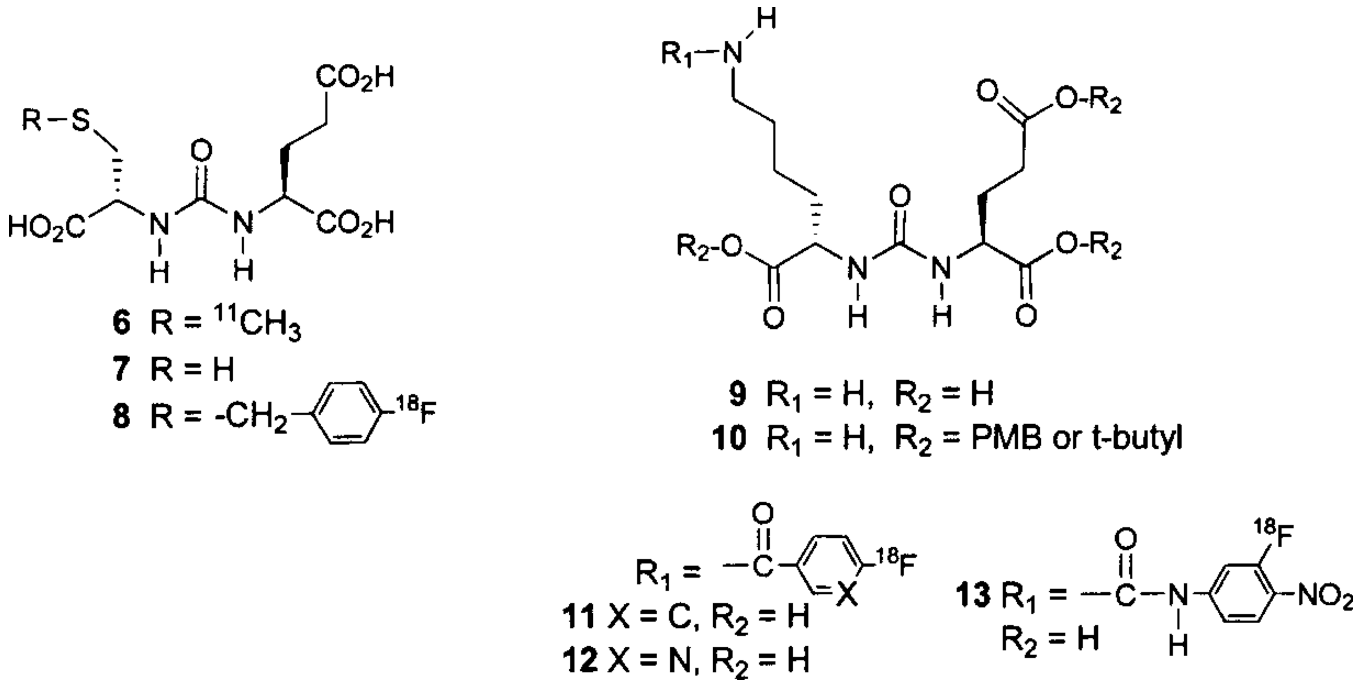

Fig. 2.
Cysteine-glutamate- and lysine-glutamate-urea-based PET radiotracers.

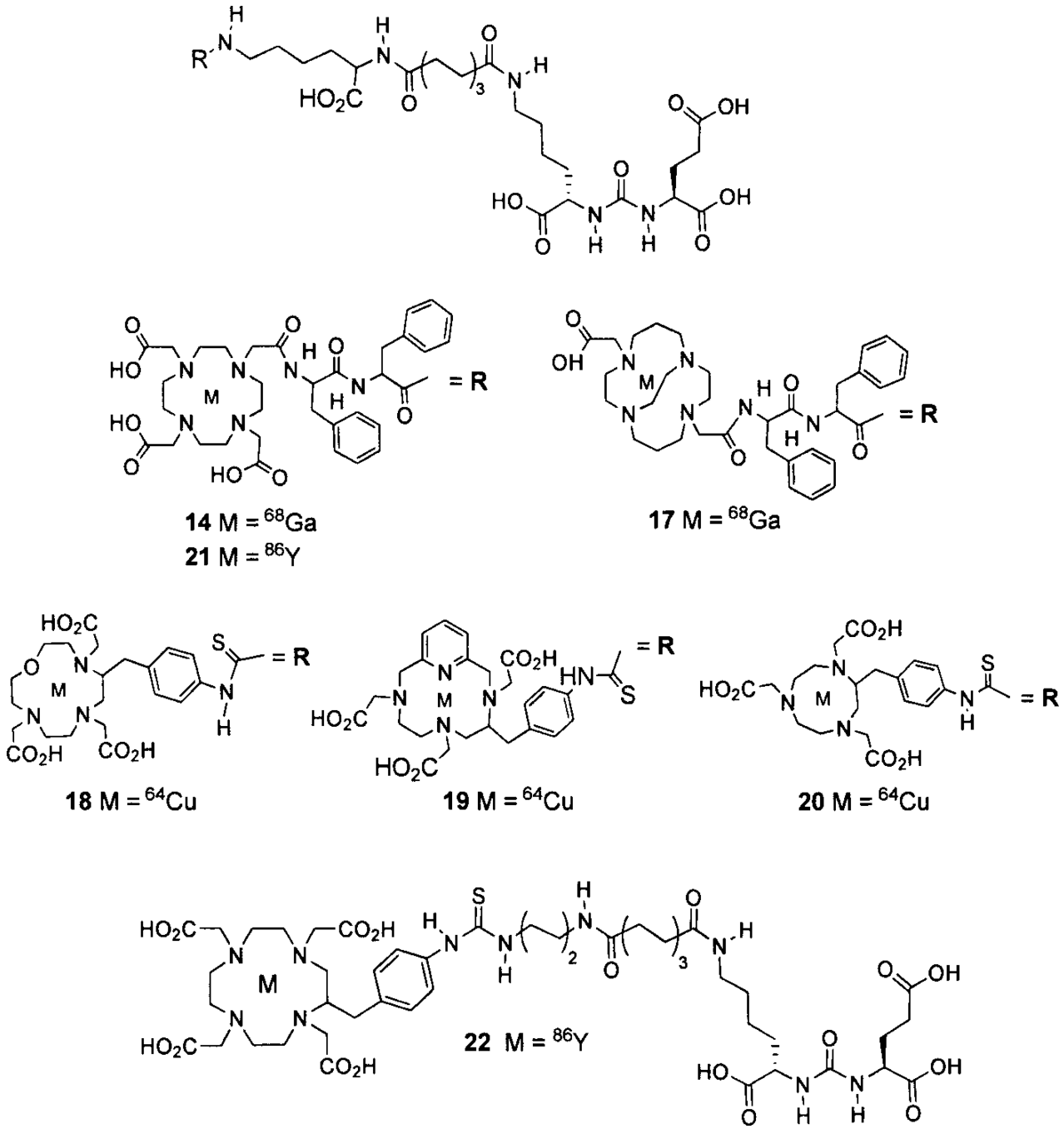

Fig. 3.
Radiometal-labeled lysine-glutamate-urea PET radiotracers.

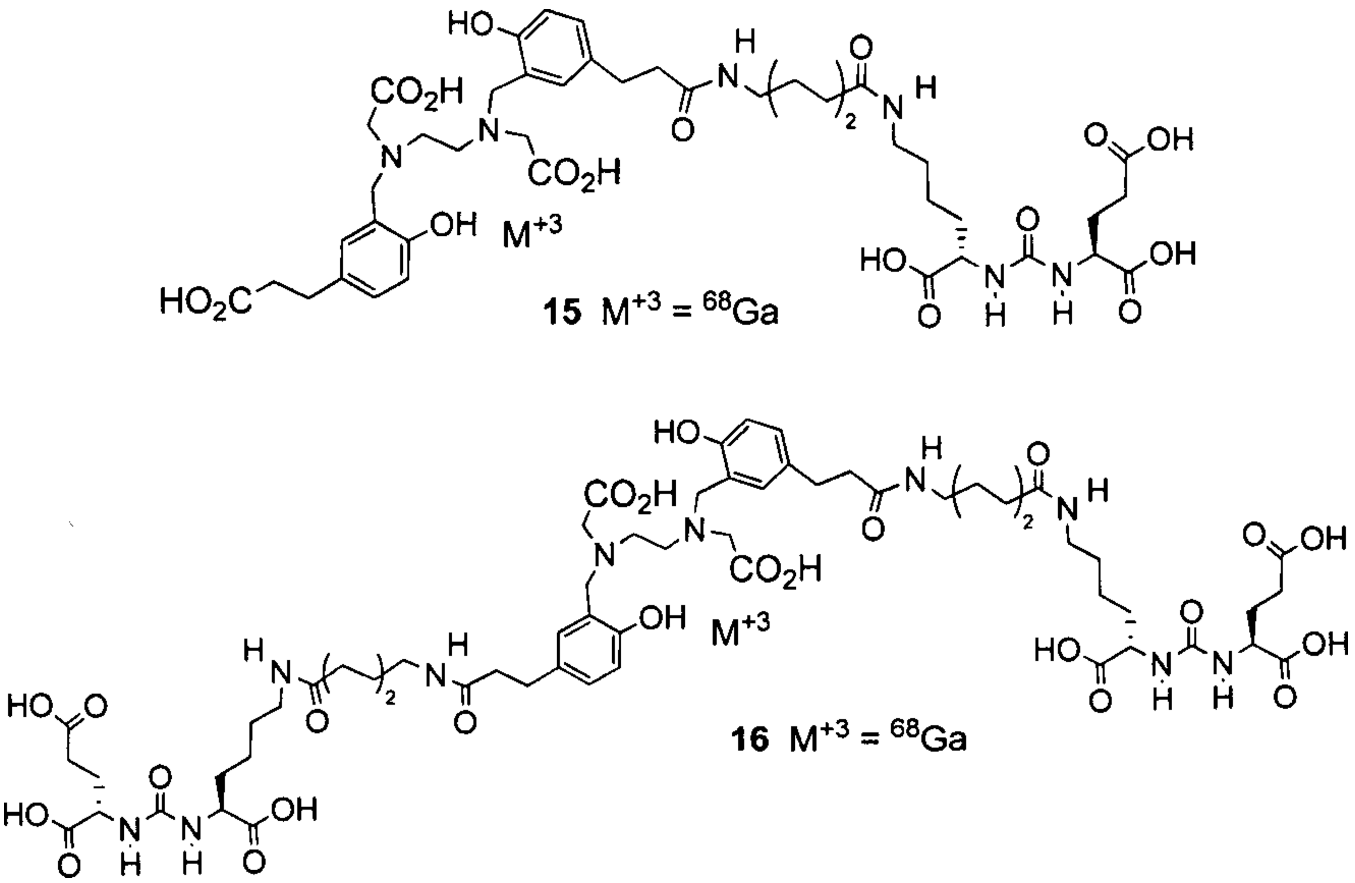

Fig. 4.
^{68}Ga-labeled HBED-CC conjugates of lysine-glutamate-urea.

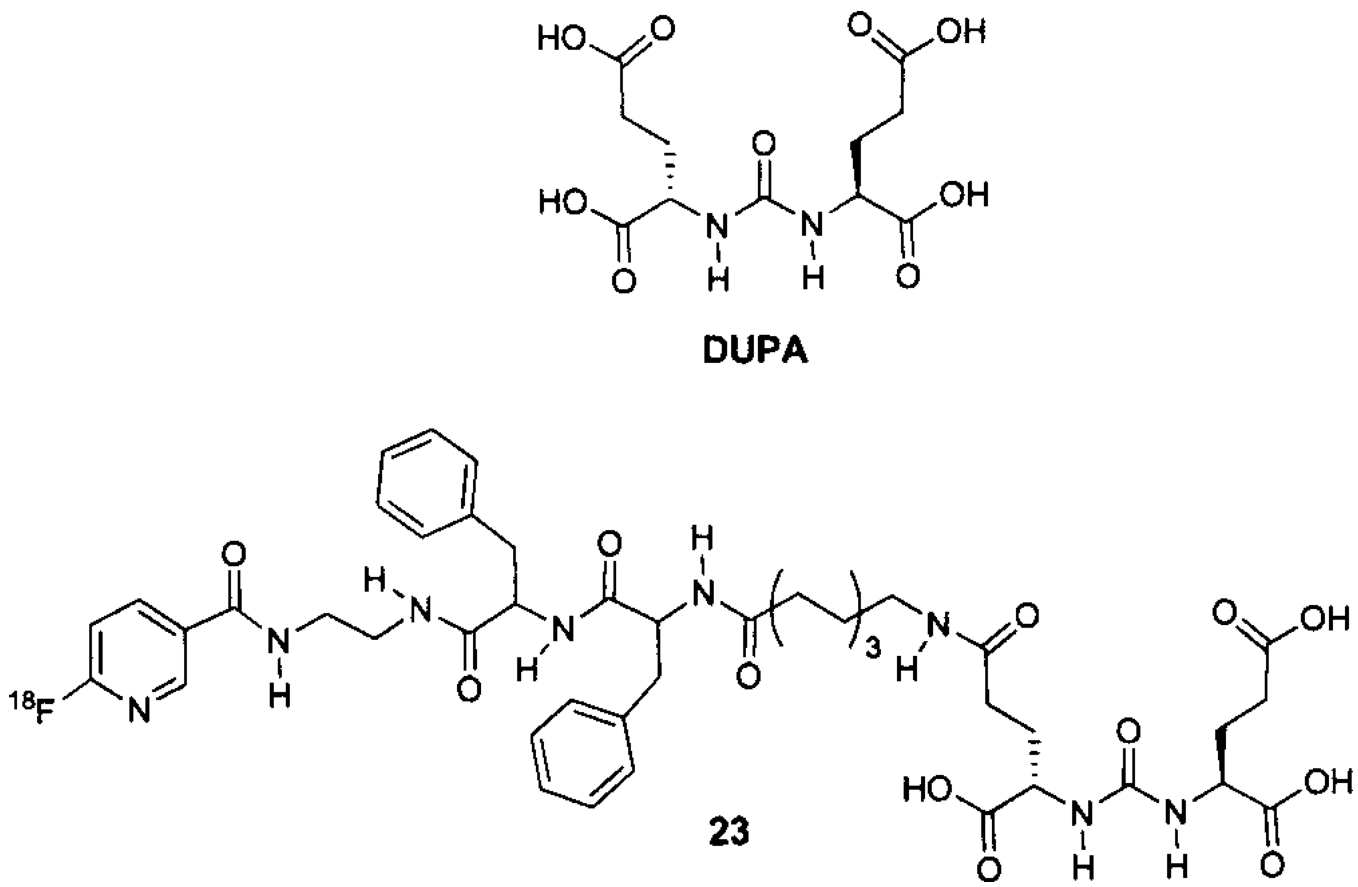

Fig. 5.
^{18}F-labeled DUPA analogs.

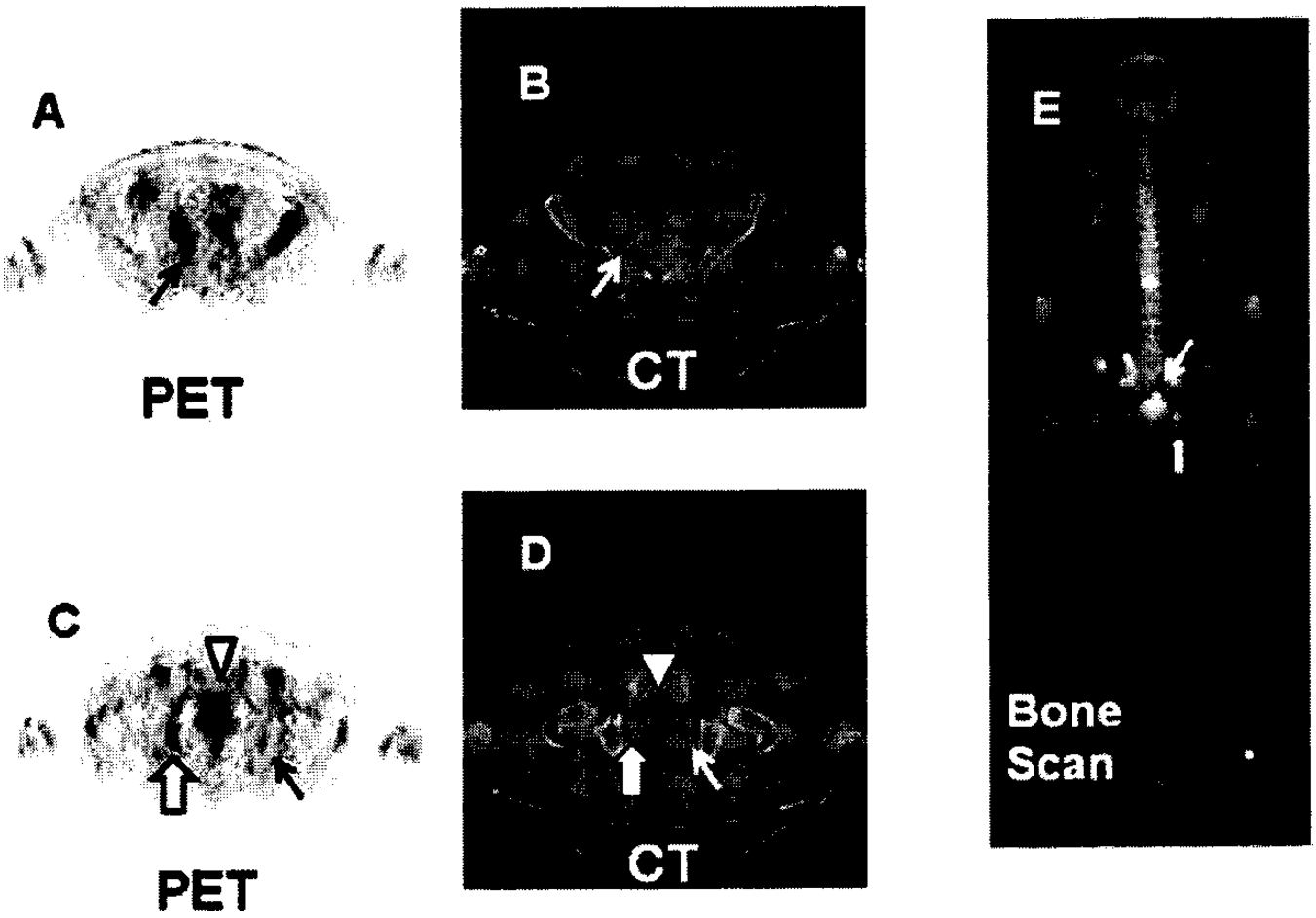

Fig. 6.

^{18}F-DCFBC PET, CT and bone scan of a patient with suspected bone metastases in the sacrum (A and B) and right and left ischium (C and D). Bone metastasis in the sacrum is located by the black arrow in A (PET) and confirmed by the arrow in E (bone scan). Bone metastasis in the right ischium is located by the bold arrow in C (PET), and E (bone scan). A smaller focus of radioactivity in the left ischium is located by the black arrow in C (PET), but is not visible on the bone scan. The arrow head in C and D denotes bladder radioactivity.

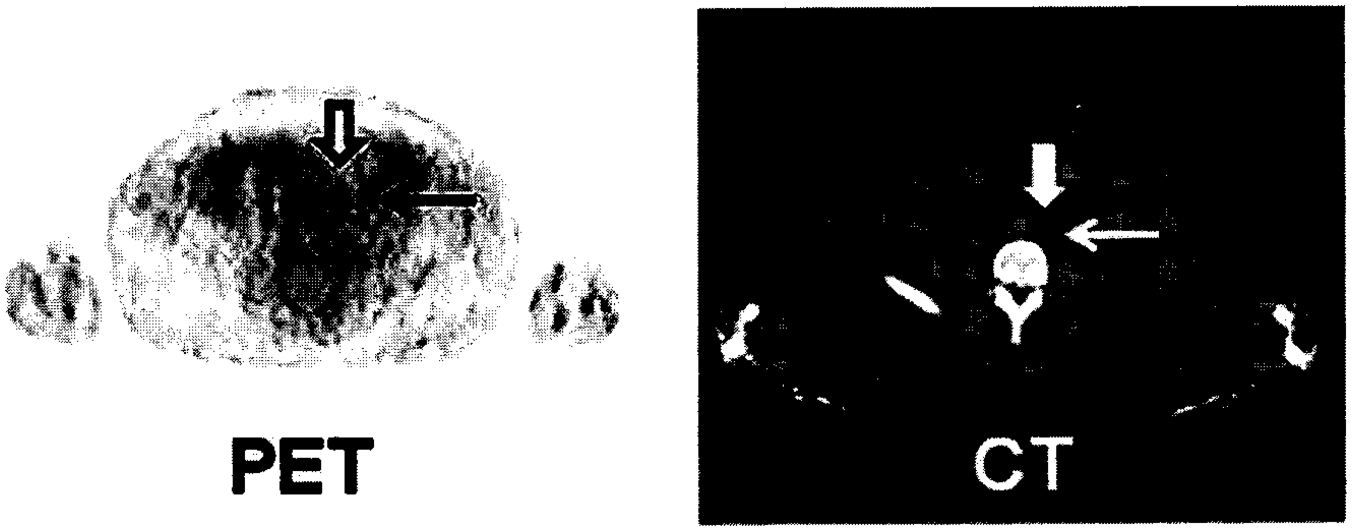

Fig. 7.

^{18}F-DCFBC PET and CT scans of a subcentimeter left common iliac lymph node. The lymph node is indicated by the bold arrow on the PET image. The lymph node is clearly discernible from urinary radioactivity in the left ureter (thin arrows on images).